

**Figure S1.** The reported bridging modes of the  $\text{CO}_3^{2-}$  ion, as obtained from a search of the Cambridge Structural database (CSD), December 2013.

## Experimental Procedures

### $[\text{Gd}_6\text{Cu}_3(\text{OH})(\text{pdm})_3(\text{O}_2\text{C}^t\text{Bu})_9(\text{CO}_3)_4(\text{MeOH})_3]$ (**1**)

$\text{Cu}(\text{NO}_3)_2 \cdot 2.5\text{H}_2\text{O}$  (0.058 g, 0.25 mmol),  $\text{Gd}(\text{NO}_3)_3 \cdot 6\text{H}_2\text{O}$  (0.226 g, 0.50 mmol), pyridine-2,6-dimethanol (0.035 g, 0.25 mmol) and  $\text{NaO}_2\text{C}^t\text{Bu}$  (0.124 g, 1.0 mmol) were dissolved in methanol (20  $\text{cm}^3$ ).  $\text{NEt}_3$  (0.14  $\text{cm}^3$ , 1.0 mmol) was added and the mixture stirred for 5 minutes. The sample was filtered and  $\text{CO}_2$  gas was then bubbled through the filtrate for 1 minute. Slow evaporation of the solution resulted in large, X-ray quality blue crystals after 3 days. Yield = 0.098 g, 39%. Calculated (found) for **1**: C, 31.43 (31.43); H, 4.53 (4.56); N, 1.48 (1.52). FT-IR:

3301 (w, br), 2962 (w), 1574 (s), 1557 (s), 1482 (s), 1423 (s), 1374 (s), 1361 (s), 1226 (m), 1094 (w), 1071 (m), 1028 (m), 896 (m) 840 (m), 805 (m), 794 (m) 755 (w), 655 (m)  $\text{cm}^{-1}$  (s = strong, m = medium, w = weak, br = broad).

### **[Y<sub>6</sub>Cu<sub>3</sub>(OH)(pdm)<sub>3</sub>(O<sub>2</sub>C<sup>t</sup>Bu)<sub>9</sub>(CO<sub>3</sub>)<sub>4</sub>(MeOH)<sub>3</sub>] (2)**

Procedure as for complex **1**, replacing Gd(NO<sub>3</sub>)<sub>3</sub>·6H<sub>2</sub>O with Y(NO<sub>3</sub>)<sub>3</sub>·6H<sub>2</sub>O (0.192 g, 0.5 mmol). Calculated (found) for **2**: C, 36.55 (36.62); H, 4.83 (4.87); N, 1.75 (1.84).

### **Crystal data and structure refinement**

Crystallographic data for **1**. C<sub>73</sub>H<sub>111</sub>Cu<sub>3</sub>Gd<sub>6</sub>N<sub>3</sub>O<sub>40</sub>, Mr = 2804.77, Trigonal, *P*-3c1, a = 22.2578(15) Å, b = 22.2578(15) Å, c = 26.9738(18) Å,  $\alpha = \beta = 90^\circ$ ,  $\gamma = 120^\circ$ , V = 11572.8(13) Å<sup>3</sup>, Z = 4, D<sub>c</sub> = 1.610 Mg/m<sup>3</sup>,  $\mu = 3.996 \text{ mm}^{-1}$ , T = 100 K; 74053 collected reflections, 8821 unique (R<sub>int</sub> = 0.0302). The final R<sub>1</sub> (I > 2 $\sigma$ (I)) = 0.0329, wR<sub>2</sub> (I > 2 $\sigma$ (I)) = 0.0910. The goodness of fit on F<sup>2</sup> = 1.053. CCDC depository number = 916293.

X-ray data was collected using Rigaku AFC12 goniometer equipped with an enhanced sensitivity (HG) Saturn724+ detector mounted at the window of an FR-E+ SuperBright molybdenum rotating anode generator with VHF Varimax optics (70 $\mu$ m focus).<sup>1</sup> Cell determination and data collection employed CrystalClear-SM Expert 2.0.<sup>2</sup> The crystal structure was solved by direct methods and full-matrix least-squares refinement on Fo<sup>2</sup> was carried out using SHELX-97 software package.<sup>3</sup> All non-hydrogen atoms were refined with anisotropic displacement parameters. All hydrogen atoms were added at calculated positions and refined using a riding model with isotropic displacement parameters based on the equivalent isotropic displacement parameter (U<sub>eq</sub>) of the parent atom. In the crystal structure two tBuCOO<sup>-</sup> groups and one coordinated MeOH molecule exhibit positional disorder which has been modelled over two sites with approximately 60:40 ratio. For disordered components vibrational restraints (SIMU/DELU), similar displacement restraints (EADP) and same distance restraints (DFIX) were used to maintain sensible geometries and atomic displacement ellipsoids. ISOR restraint was necessary to restrain C9B, to have approximate isotropic behaviour. Approximately 21% of the unit cell volume comprises a large region of diffused disordered solvent which could not be modelled as discrete atomic sites. SQUEEZE<sup>4</sup> routine of PLATON<sup>5</sup> was applied to remove the contributions to the structure factors from the solvent molecules. This also improves model and good

convergence was obtained at the end of the structure refinement. A relatively large residual density peak ( $\sim 6\text{e}/\text{\AA}^3$ ) 4.64  $\text{\AA}$  away for Gd1 and 4.50  $\text{\AA}$  away from Gd2 corresponds possibly to the another Gd atom (6%) originating from crystal impurity (small crystal grown on the main crystal surface) or small twin domain which contributes to the diffraction pattern intensities.

Crystallographic data for **2**.  $\text{C}_{73}\text{H}_{115}\text{Cu}_3\text{N}_3\text{O}_{40}\text{Y}_6$ , Mr = 2398.75, Trigonal,  $P\text{-}3\text{c}1$ ,  $a = 22.1594(5)$   $\text{\AA}$ ,  $b = 22.1594(5)$   $\text{\AA}$ ,  $c = 27.1020(7)$   $\text{\AA}$ ,  $\alpha = \beta = 90^\circ$ ,  $\gamma = 120^\circ$ ,  $Z = 4$ ,  $D_c = 1.382$   $\text{Mg}/\text{m}^3$ ,  $\mu = 3.596$   $\text{mm}^{-1}$ ,  $T = 120$  K. A total of 61513 collected reflections, of which 7049 were unique ( $R_{\text{int}} = 0.1025$ ). The final  $R_1 (I > 2\sigma(I)) = 0.0615$ ,  $wR_2 (I > 2\sigma(I)) = 0.1676$ . The goodness of fit on  $F^2 = 1.032$ . CCDC depository number = 939977.

X-ray data was collected on an Agilent Technologies SuperNova diffractometer with an Atlas CCD detector using Mo-K $\alpha$  radiation ( $\lambda = 0.71073$   $\text{\AA}$ ) and a crystal temperature of 120 K. A face-indexed absorption correction was applied using *CrysAlisPro*.<sup>6</sup> The structure was solved by charge flipping using Superflip<sup>7</sup> and full-matrix least-squares refinement was carried out using SHELXTL.<sup>3</sup> C-bound H atoms were placed in calculated positions and refined with constrained C—H geometry. The O-bound H atom was identified from a difference Fourier map and refined with the O—H distance restrained to 0.84(1)  $\text{\AA}$  and  $U_{\text{iso}}(\text{H}) = 1.2 U_{\text{eq}}(\text{C})$ . The asymmetric unit of **2** lies on a three-fold rotation axis which passes through O14 and C24. One pivalate ligand (O5 to C17) was modelled over two sites with refined occupancy ratio 0.513:0.487(15) using isotropic similarity restraints on all atoms. C16 and C16' were constrained to share the same coordinates and displacement ellipsoid (refinement would otherwise not converge). The methanol ligand was also refined as disordered (0.50:0.50(5)). Several large residual peaks remain in a difference map, in positions which are chemically unreasonable to be overlooked. The largest is 4.24  $\text{e}/\text{\AA}^3$  located 0.85  $\text{\AA}$  from H15E. Residual twinning does not seem to be the cause. Structure **1** suffers from virtually the same problems (disorder, large residual electron density). There is as a result a large void of 1085  $\text{\AA}^3$  reported by PLATON/checkCIF. In the case of **2** the identity of the residual peaks could not be established chemically and is not appropriate to remove them with SQUEEZE.

1. S. J. Coles and P.A. Gale, *Chem. Sci.*, **2012**, *3*, 683.
2. CrystalClear-SM Expert 2.0 r11 (Rigaku, 2011).

3. SHELXL97 (G. Sheldrick, G.M. (2008). *Acta Cryst.*, *A64*, 112.
4. SQUEEZE - P. v.d. Sluis and A. L. Spek, *Acta Cryst.*, **1990**, *A46*, 194.
5. PLATON/PLUTON - (a) *J. Appl. Cryst.*, **2003**, *36*, 7; (b) A. L. Spek, *PLATON. A Multipurpose Crystallographic Tool*. Utrecht University, The Netherlands (2002).  
<http://www.cryst.chem.uu.nl/platon>
6. CRYCALISPRO - Agilent Technologies, (2011), *CrysAlisPro*, Agilent Technologies UK Ltd, Oxford, UK
7. L. Palatinus and G. Chapuis, *J. Appl. Cryst.*, **2007**, *40*, 786-790.

### Magnetic and heat capacity measurements

The magnetic data were collected on a MPMS-XL SQUID magnetometer equipped with a 5 T magnet. DC susceptibility data were obtained with  $B = 0.1$  T in the temperature range 1.8–300 K (Fig. 3), while isothermal magnetization curves were measured for selected temperatures below 10 K (Fig. S2). MagPack was used for fitting the susceptibility data to the spin Hamiltonian, as described in the main text. Heat capacity ( $C$ ) measurements (Fig. S3, top panel) were carried out for complex **1** at temperatures down to 0.3 K by using a 14T-PPMS, equipped with a  $^3\text{He}$  cryostat. The experiment was performed on a thin pressed pellet ( $\sim 1$  mg) of polycrystalline sample thermalized by  $\sim 0.2$  mg of Apiezon N grease, whose contribution was subtracted by using a phenomenological expression. Using the equation  $S(T) = \int C/T \, dT$ , the temperature-dependence of the entropy  $S$  is obtained and depicted in Figure S3, bottom panel. The MCE, reported in Figure 4, is thus evaluated by obtaining straightforwardly the isothermal magnetic entropy changes  $-\Delta S_m(T)$ , following a change in the applied magnetic field  $\Delta B$  (cf. the top panel). Similarly, we obtain the adiabatic temperature change,  $\Delta T_{\text{ad}}$ , depicted in the bottom panel.

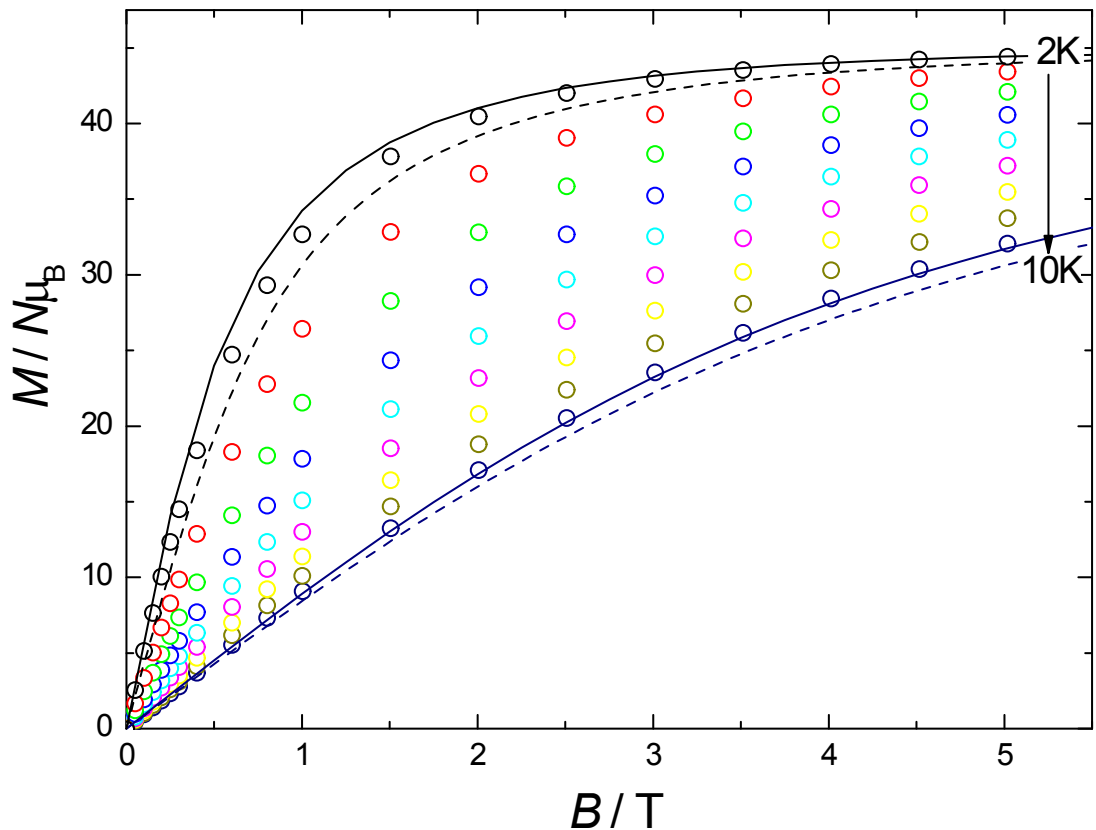


**Figure S2.** Isothermal magnetization data of  $\text{Gd}_6\text{Cu}_3$  for  $T = 2 - 10$  K, step 1 K. Solid lines are calculations for  $T = 2$  and 10 K, respectively, as obtained by using the same parameters found from the best fit of the susceptibility, i.e.,  $J_{\text{Cu-Cu}} = 0.87$  K and  $J_{\text{Gd-Cu}} = 0.40$  K. Dashed lines are Brillouin functions for  $T = 2$  and 10 K, respectively, for six  $\text{Gd}^{\text{III}}$  and three  $\text{Cu}^{\text{II}}$  paramagnetic ions, as comparison.

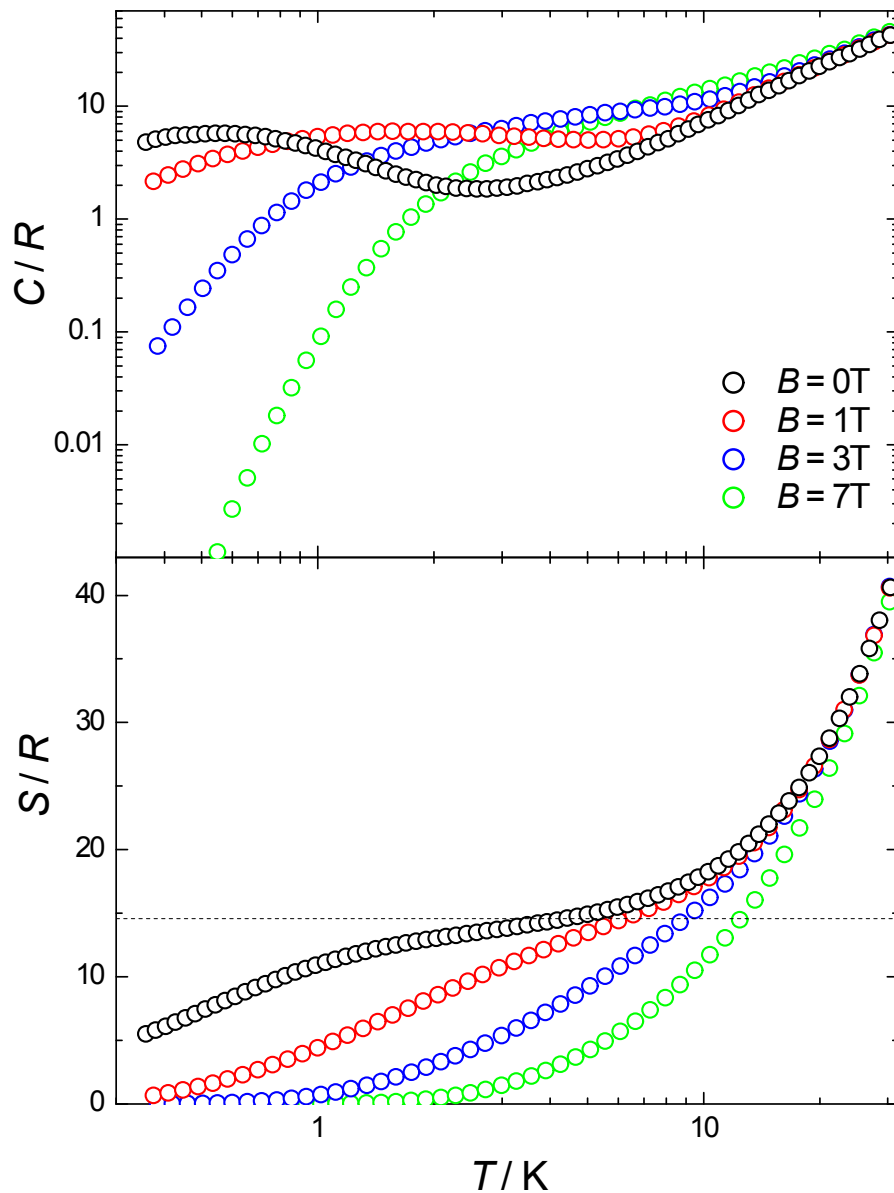


**Figure S3.** Molar heat capacity of **1**, normalised to the gas constant  $R$ , vs  $T$  for several applied fields, as labelled (top panel). Molar entropy, normalised to  $R$ , vs  $T$ , as obtained from the heat capacity data at the corresponding fields (bottom). Dashed line is the full magnetic entropy content corresponding to six  $\text{Gd}^{\text{III}}$  and three  $\text{Cu}^{\text{II}}$  non-interacting ions, *i.e.*,  $S/R = 6\ln(2s_{\text{Gd}}+1)+3\ln(2s_{\text{Cu}}+1) = 14.56$ , where  $s_{\text{Gd}} = 7/2$  and  $s_{\text{Cu}} = 1/2$ .